IEEE Access
Multidisciplinary | Rapid Review | Open Access Journal

Date of publication xxxx 00, 0000, date of current version xxxx 00, 0000.

Digital Object Identifier 10.1109/ACCESS.2020.Doi Number

Coverage-Aware Recharging Scheduling Using Mobile Charger in Wireless Sensor Networks

Bhargavi Dande[1], Shi-Yong Chen[1], Huan-Chao Keh[1], Shin-Jer Yang[2] and Diptendu Sinha Roy[3]

[1]Department of Computer Science and Information Engineering, Tamkang University, New Taipei City 25137, Taiwan
[2]Department of Computer Science and Information Management, Soochow University, Taipei City 11102, Taiwan
[3]Department of Computer Science and Engineering, National Institute of Technology Meghalaya, Shillong 793003, India

Corresponding author: Huan-Chao Keh (e-mail: hckeh@mail.tku.edu.tw).

ABSTRACT Energy recharging in wireless rechargeable sensor networks (WRSNs) has acquired much attention in recent years. In literature, many recharging path construction algorithms have been proposed. Most of them considered that all sensors are equally important and designed algorithms to increase the number of recharged sensors or decrease the path length of the mobile charger. However, different sensors have different coverage contributions. Recharging the sensors with larger coverage contribution can achieve better surveillance quality. The proposed recharging scheduling algorithm is divided into three phases, including the *Initialization*, *Recharging Scheduling and Path Construction Phases*. In the second phase, this paper proposed two recharging scheduling algorithms, namely the *Cost-Effective* (*CE*) *algorithm* and *Cost-Effective with Considerations of Coverage and Fairness* (C^2F) *algorithm*. The proposed two algorithms construct paths for the mobile charger and select the recharging sensors based on the higher weight in terms of larger coverage contribution and smaller path cost. Performance results show that the CE and C^2F algorithms yield better performance in terms of the fairness of recharging, recharging stability and coverage ratio, as compared with the existing studies.

INDEX TERMS mobile charger, recharging, coverage, wireless sensor networks, ping-pong effect

I. INTRODUCTION

Wireless sensor networks (WSNs) are used in numerous applications like border surveillance [1], smart homes [2], precision agriculture [3] and environmental monitoring [4]. In general, the WSNs can monitor the specified events and report the data if any event occurs in their location. Even though WSNs are broadly used, the finite energy of the sensors is still one of the major challenges, which need to be further improved. To solve the energy constraint issue in WSNs, many algorithms have been designed in the literature. These studies can be categorized into two classes: energy preservation [5]-[8] and energy replenishment [9]-[19] technologies.

Studies [5]-[8] designed algorithms to reduce the energy consumption of the sensors in the network. Although these studies aimed to extend the lifetime of WSNs, they cannot recompense the energy exhaustion of sensors. On the other hand, energy replenishment technologies [9]-[19] can recharge the sensors based on the energy collected from environmental resources or radio-frequency energy transmission. These studies are further divided into two classes, including environmental energy [9]-[11] and mobile chargers [12] - [19].

In the first class, many algorithms were proposed by considering the environmental energy harvesting systems [9]-[11]. All of these studies assumed that the energy of sensors can be collected from environmental energy resources like solar, wind and thermal energies. Although the scale of environmental resources was extensive, they were unpredictable. These resources highly depended on various parameters such as time and weather, which indicated that environmental resources were unstable.

To overcome the unpredictable and unstable issues, many algorithms considered radio-frequency energy transmission mechanisms [12]-[19], which are categorized into the second class. These studies assumed that the radio-frequency signals transmitted by mobile chargers would transmit the energy beacons to the sensors. Most of them considered the static sensors and assumed that the mobile charger will traverse the network aiming to recharge all sensors. In general, the energy of the mobile charger was also finite, thereby the sink was considered as the energy station, which supplied energy to the

This article has been accepted for publication in a future issue of this journal, but has not been fully edited. Content may change prior to final publication. Citation information: DOI 10.1109/ACCESS.2021.3088524, IEEE Access

mobile charger in the network. Therefore, the radio-frequency energy transmission algorithms can be applied to recharge the sensors in an efficient and balanced way compared to the environmental resources. However, given a set of sensors and a mobile charger, determining some recharging locations to construct an efficient path for the mobile charger is still a big challenge.

This paper proposed two recharging scheduling algorithms, namely the *CE* and C^2F *algorithms*. These algorithms construct paths for the mobile charger, aiming at maximizing the surveillance quality of the whole monitoring area. To avoid the *ping-pong effect*, the proposed C^2F algorithm adopts the *charging fairness policy*, which locks the sensors that have been recharged recently. In addition, the proposed algorithm considers the c*hain-effect*. Since recharging one sensor can increase the latency of energy recharging for the other waiting sensors. This can cause much energy consumption of the waiting sensors and might lead to energy exhaustion of these sensors, resulting in coverage loss. Therefore, the recharging schedule has a *chain-effect*, which impacts the monitoring quality. The proposed algorithm takes into account the *chain-effect* and calculates the coverage loss and benefits of each candidate charging location, aiming to maximize the monitoring quality. The following details the key contributions of the proposed algorithm.

(1) ***Avoiding the ping-pong effect***: This paper partitions the whole region into grids to decrease the complexity. The mobile charger always chooses the best grid for executing the recharging task. By considering the fairness of recharging the sensors, the previous charged time of the sensor is taken into account. Compared to the existing works [14-19], the proposed algorithms avoid the ping-pong effect caused by the movement of the mobile charger.

(2) ***Achieving better surveillance quality:*** Most existing studies considered that each sensor is equally important in the coverage contribution. The proposed energy-recharging algorithm calculates the contribution of each sensor and recharges the sensors with larger coverage contribution. This strategy achieves better surveillance quality, as compared with the existing studies [18] and [19].

(3) ***Maintaining unlimited lifetime:*** The proposed energy-recharging algorithm can maintain the unlimited lifetime of the given sensor network. This can be achieved because that the sensor plays an important role in terms of coverage contribution will be recharged efficiently to prevent it from energy exhaustion, maintaining its perpetual lifetime.

(4) ***Considering the impact of chain-effect on monitoring quality:*** Compared to the existing studies [17-19], the proposed algorithm considers the c*hain-effect*. The proposed C^2F algorithm calculates the coverage loss and benefits of each sensor which is waiting for recharging and makes a recharging schedule, aiming to maximize the monitoring quality.

The remaining part of the paper is structured as follows. The existing studies of the mobile charger scheduling issue are reviewed in Section II. The preliminaries of the considered scenario and problem statement are detailed in Section III. Section IV presents the design of the proposed *CE* and C^2F algorithms. Section V compares the performance results of *CE* and C^2F with the existing algorithms. In the end, the conclusion is given in Section VI.

II. RELATED WORK

In this section, the literature of energy replenishment technology is presented. These studies are divided into two types: environmental energy [9]-[11] and mobile chargers [12] - [19]. The following subsections review the studies related to this work.

A. ENERGY REPLENISHMENT FROM ENVIRONMENTAL ENERGY

In this category, most of the existing studies [9]-[11] adopted the environmental energy harvesting technologies like solar, wind and thermal energies to maintain the perpetual lifetime of WSNs. Study [9] considered the solar energy harvesting system for a rechargeable WSN. The voltage is harvested from the sunlight by using solar panels. The solar panel converted light energy directly into electrical energy and recharged the battery. However, the environmental resources were unpredictable and depended on various parameters such as time and weather, which indicated that environmental resources were unstable.

In the environmental energy resources, wind energy was also one of the supplementary energy systems, which have been widely used in past years. Peng et al. [10] proposed a fault detection method for wind turbine monitoring based on the WSN. Another study [11] utilized three kinds of wind, solar and thermal energy harvesters and combined them as electric power. Finally, the WSN nodes can be recharged using a super capacitor. However, the wind energy harvesting system cannot acquire enough energy and the size of the wind turbine generator might lead to deployment issues. On the other hand, the construction of the thermoelectric generator was complicated and it consumed more energy compared to the solar harvesting systems.

B. ENERGY REPLENISHMENT FROM MOBILE CHARGERS

The second category is the energy replenishment from mobile chargers. Many studies [12-19] were proposed in the past few years to optimize the charging algorithms, which can prolong the lifetime of WSNs. Study [12] proposed a novel clustering scheme, which elected few nodes as the cluster heads. The moving vehicle was assumed to recharge only the cluster heads as well as collect data from them. Thereby, the utility of the WSNs was maximized. However, they did not consider the finite energy of the moving vehicle. To address

This article has been accepted for publication in a future issue of this journal, but has not been fully edited. Content may change prior to final publication. Citation information: DOI 10.1109/ACCESS.2021.3088524, IEEE Access

this issue, Lyu et al. [13] designed an algorithm assuming the finite energy of mobile charger. In this study, the problem of periodic charging guaranteed that the energy of sensor nodes varied periodically, thus they can maintain the perpetual lifetime of these sensor nodes.

Study [14] proposed a joint charging and scheduling algorithm by using a mobile charger. This study investigated two issues, the first one was deciding the charging sensors and their charging time while the second one was scheduling the sensors based on their received energy. Another study [15] proposed a partial charging algorithm, aiming to recharge the sensors partially in the network. They also investigated the scheduling problem of the mobile charger. Study [16] proposed a recharging algorithm, aiming to design an energy-efficient traveling path for multiple mobile chargers. In this study, the whole network was divided into many sub-regions to maximize the benefit of multiple mobile chargers. Then the charging radius based nearest neighbor approach was applied to find the charging points, which improved the charging efficiency. However, they ignored that different sensors have different contributions in terms of the monitoring quality. Similar to the study [16], another study [17] partitioned the network aiming to equally distribute the workload to each mobile charger. Then fuzzy logic was applied to determine the charging schedule of the mobile chargers. Besides, this study considered the adaptive threshold for charging requests, aiming to recharge the nodes with different energy consumption rates.

The Spatial Dependent Task Scheduler (SDT) algorithm [18] focused on the different energy consumption rates of sensors, aiming to increase the number of nodes alive for monitoring purposes. Study [19] proposed an algorithm, called HSA-DFWA, for recharging the multi-node using a mobile charger in WRSNs. This study assumed the real scenarios of the mobile charger and proposed three models of charging plans and algorithms.

Although the mechanisms proposed in [12-19] improved the charging strategy of the mobile charger in different ways, they did not consider the coverage contribution of sensors. Table 1 summarizes the comparison of the proposed and related studies. This paper proposed a recharging scheduling algorithm based on radio-frequency energy transmission technology. The objective of this study is to maximize the accumulated monitoring quality of all sensors in the given network. The proposed *CE* and C^2F *algorithms* construct paths for the mobile charger, aiming at maximizing the surveillance quality of the whole monitoring area. The proposed *CE algorithm* considers the maximal lifetime policy while the C^2F *algorithm* considers the fairness recharging policy. Both the proposed *CE* and C^2F *algorithms* avoid the ping-pong effect caused by the movement of the mobile charger.

TABLE I.
COMPARISON OF THE PROPOSED AND RELATED WORKS.

Related work	Considering coverage contribution	Dynamic scheduling	Charging stability	Avoiding the ping-pong effect
[9]	×	×	×	×
[10]	×	×	×	×
[11]	×	×	×	×
[12]	×	×	○	×
[13]	×	×	○	×
[14]	×	×	○	×
[15]	×	×	○	×
[16]	×	○	○	×
[17]	○	○	○	×
[18]	×	○	○	×
[19]	○	×	○	×
The proposed algorithm	○	○	○	○

III. NETWORK MODEL AND PROBLEM FORMULATION

The following subsections will firstly introduce the considered environment of the proposed algorithm. Then the problem formulation and the objective function are proposed.

A. NETWORK MODEL

Assume that a given WSN comprises a set of n sensors $S = \{s_1, s_2, \dots, s_n\}$ deployed in a region A. The energy of all sensors is limited and their energy consumption rates are different.

It is assumed that a single mobile charger M traverses in A with constant speed v. Let $E_{charger}^{total}$ represent the total energy of M. Let L_{max} represent the path length of M. In the total observing time T, the M can only move L_{max} to perform the charging task. Based on these assumptions, this paper develops a scheduling algorithm for M to determine some recharging locations, aiming to recharge the sensors such that the monitoring quality Q of the whole network can be maximized.

This article has been accepted for publication in a future issue of this journal, but has not been fully edited. Content may change prior to final publication. Citation information: DOI 10.1109/ACCESS.2021.3088524, IEEE Access

B. PROBLEM FORMULATION

Let the total observing time T is separated into m time slots $T=\{t_1, t_2, \dots t_j, \dots t_m\}$. Let τ denote the time slot length. Let a_i denote the sensing area of the sensor s_i. Let Q^j represent the monitoring quality at time slot t_j, which is the size of the covered area by sensor set S in a time slot t_j. Let r_{crg} denote the charging range of each sensor. The sensor s_i can be charged by M only if M is located in the r_{crg} of the sensor s_i. Let $l_{current}$ and l_i denote the current location of M and the location of the sensor s_i, respectively. Let $d(l_i, l_{current})$ represent the distance between s_i and M. Let $\varphi_{i,j}^c$ be a Boolean variable indicating either M is located in the r_{crg} of the sensor s_i at time slot t_j.

$$\varphi_{i,j}^c = \begin{cases} 1 & d(l_i, l_{current}) \le r_{crg} \\ 0 & d(l_i, l_{current}) > r_{crg} \end{cases} \quad (1)$$

Let E_i^{crg} represent the energy of the sensor s_i charged by M. Let P_{crg}^{tx} represents the transmission power of M and z_{crg}^{tx} and z_{crg}^{rx} are the transmitter and receiver antenna gains, respectively. The Friis transmission equation [20] is adopted to calculate the recharged energy E_i^{crg} obtained by receiver s_i as shown in Exp. (2).

$$E_i^{crg} = P_{crg}^{tx} \times \left(\frac{\lambda_{crg}}{4\pi(d(l_i, l_{current})) + \beta_{crg})} \right)^2 \times \frac{z_{crg}^{tx} \times z_{crg}^{rx} \times \sigma_{crg}}{\psi_{crg}} \quad (2)$$

The notation λ_{crg} denotes the wavelength of the radio-frequency wave and σ_{crg} denotes the rectifier efficiency. Finally, ψ_{crg} denotes the polarization loss. Let $\xi_{i,j}^{crg}$ be the Boolean variable indicating whether or not the sensor s_i is charged by M at time slot t_j.

$$\xi_{i,j}^{crg} = \begin{cases} 1 & if\ sensor\ s_i\ charged\ at\ t_j \\ 0 & otherwise \end{cases} \quad (3)$$

Let $E_{i,j}^{crg}$ represent the charged energy of the sensor s_i at time slot t_j. Exp. (4) gives the derivation of $E_{i,j}^{crg}$.

$$E_{i,j}^{crg} = \int_0^\tau \varphi_{i,j}^c \times E_i^{crg} dt \ \forall\ t_j \in T, s_i \in S \quad (4)$$

Let E_i^{con} represent the energy consumed by the sensor s_i for executing sensing and communication tasks. Let $E_{i,j}^{rem}$ represent the remaining energy of the sensor s_i at time slot t_j. The notation $E_{i,j}^{rem}$ is evaluated by applying Exp. (5).

$$E_{i,j}^{rem} = E_{i,j-1}^{rem} + E_{i,j}^{crg} * \xi_{i,j}^{crg} - E_i^{con} \quad (5)$$

Let ζ denote the reserved energy required for fundamental operations of each sensor, including the energy for waking up and initializing the recharging circuit. In other words, each sensor will stay in working state only if $E_{i,j}^{rem}$ is greater than ζ. Let notation μ_i^j denote the Boolean variable indicating whether or not the sensor s_i has enough remaining energy $E_{i,j}^{rem}$ for executing sensing task at a time slot t_j. That is,

$$\mu_i^j = \begin{cases} 1 & if\ E_{i,j}^{rem} \ge \zeta \\ 0 & otherwise \end{cases} \quad (6)$$

The monitoring quality at the time slot t_j is evaluated as shown in Exp. (7).

$$Q^j = \bigcup_{i=1}^{i=n} \mu_i^j \times a_i \quad (7)$$

The accumulated monitoring quality for time period $T = [t_1, t_j]$ is represented by Φ^j as shown in Exp. (8).

$$\Phi^j = \sum_{i=1}^{j} Q^i \quad (8)$$

Recall that $T=\{t_1, t_2, \dots t_j, \dots t_m\}$ is divided into m time slots. Let Φ^m denote the accumulated monitoring quality from time period t_1 to t_m. Recall that A denotes the monitoring region. The goal of the proposed algorithm is to maximize the accumulated monitoring quality of all sensors in T over the whole monitoring region.

Objective function:

$$Max\left(\frac{\Phi^m = \sum_{j=1}^m Q^j}{A * m} \right) \quad (9)$$

Several constraints should be satisfied when achieving the goal given in Exp. (9). These constraints are related to energy recharging and consumption. Let B represent the maximum battery capacity of each sensor. Recall that ζ denotes the reserved energy required for fundamental operations of each sensor. The following constraint indicates that $E_{i,j}^{rem}$ of each sensor cannot be smaller than ζ and greater than B.

(1) Sensor Battery Constraint:

$$\zeta \le E_{i,j}^{rem} \le B, \forall t_j \in T, \forall s_i \in S \quad (10)$$

The second constraint is the charging time constraint, which restricts the charging time of each sensor. Let T_j^{crg} denote the time duration required for sensor s_j to be fully charged.

(2) Charging Time Constraint:

$$0 \le T_j^{crg} \le \frac{min(B - \zeta, B - E_{i,j}^{rem})}{E_i^{crg}} \quad (11)$$

In case M is located in the charging range of the sensor s_i which is fully recharged by M, the charged energy equals to $B - E_{i,j}^{rem}$. On the contrary, if M is far away from the sensor s_i, sensor s_i cannot be recharged. Therefore, the additional energy of the sensor s_i obtained from M cannot be larger than

This article has been accepted for publication in a future issue of this journal, but has not been fully edited. Content may change prior to final publication. Citation information: DOI 10.1109/ACCESS.2021.3088524, IEEE Access

$min\left(B-\zeta, B-E_{i,j}^{rem}\right)$. Thus the charging time constraint should be satisfied.

The final constraint is the path length constraint. The total path length that M can move is limited. Recall that L_{max} denote the maximal path length that M can move during time period T. Let α denote the energy consumption rate of M during its movement. The maximal time length for the movement of M is L_{max}/v. Let E^{move} represent the total energy consumption of M moving with length L_{max}. Exp. (12) calculates the value of E^{move}.

$$E^{move} = \alpha \times \frac{L_{max}}{v} \tag{12}$$

Recall $E_{charger}^{total}$ denote the total energy of M. Let $E_{charger}^{con}$ represent the energy consumption of M for moving and recharging during time period T. The value of $E_{charger}^{con}$ can be obtained as shown in Exp. (13).

$$E_{charger}^{con} = \int_{0}^{L_{max}/v} P_{crg}^{tx}\, dt \tag{13}$$

Finally, the following path length constraint should be satisfied.

(3) Path Length Constraint:

$$L_{max} \leq E_{charger}^{total} - E_{charger}^{con} \tag{14}$$

IV. THE PROPOSED RECHARGING ALGORITHM

This section details the proposed recharging algorithm, which aims to maximize Φ^j of all the sensors in T. The main idea of this algorithm is that M will charge the requested sensors which have the maximal coverage contribution and minimal path cost. The proposed algorithm is divided into three phases: *Initialization Phase*, *Recharging Scheduling Phase and Path Construction Phase*. The first phase partitions the whole region into equal-sized grids. Then it calculates the sensing and recharging set for each grid $g_{x,y}$. These sets will be used in the later phases. The second phase aims to select and schedule the sensors, which have sent the charging requests to M. Finally, the third phase constructs a path for M based on the schedule of sensors in the second phase. Each phase will be detailed in the following subsections.

A. INITIALIZATION PHASE

This phase divides the whole region into several grids. A grid labeled with coordinates (x, y) represents the grid $g_{x,y}$. As depicted in Fig. 1, there are n sensor nodes randomly deployed in A. Let c_i^{sen} denote the sensing coverage of the sensor s_i. Let recharging coverage, denoted by c_i^{rcg} represent the area where M can recharge sensor s_i.

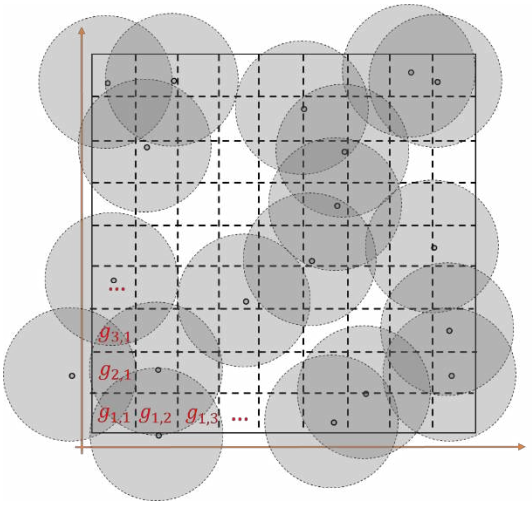

FIGURE 1. **The scenario of the considered network environment.**

Let r_{sen} represent the sensing range of each sensor. Recall that r_{crg} denote the charging range. In general, the sensing range of each sensor is larger than the charging range as shown in Fig. 2.

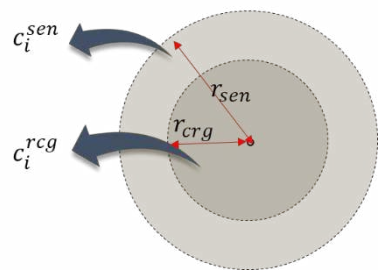

FIGURE 2. **The sensing and charging ranges of the sensor s_i.**

A grid g is said to be recharging or sensing covered by the sensor s_i if the recharging or sensing ranges of s_i cover more than the half area of $g_{x,y}$, respectively. Let $S_{x,y}^{rcg}$ denote recharging coverage set whose recharging range covers $g_{x,y}$. That is,

$$S_{x,y}^{rcg} = \{s_i | g_{x,y}\ is\ recharging\ covered\ by\ c_i^{rcg}\} \tag{15}$$

Let $S_{x,y}^{sen}$ denote the set of sensors whose sensing ranges cover $g_{x,y}$. That is,

$$S_{x,y}^{sen} = \{s_i | g_{x,y}\ is\ sensing\ covered\ by\ c_i^{sen}\} \tag{16}$$

Fig. 3 illustrates an example of relationships of $S_{x,y}^{rcg}$, $S_{x,y}^{sen}$ and $g_{x,y}$. As shown in Fig. 3, both the charging ranges of sensors s_1 and s_2 cover the half area of $g_{2,1}$. Therefore, we have $S_{2,1}^{rcg}=\{s_1, s_2\}$. Similarly, the sensing ranges of sensors s_1, s_2 and s_3 cover the half area of $g_{2,1}$. Therefore, we have $S_{2,1}^{sen} = \{s_1, s_2, s_3\}$.

This article has been accepted for publication in a future issue of this journal, but has not been fully edited. Content may change prior to final publication. Citation information: DOI 10.1109/ACCESS.2021.3088524, IEEE Access

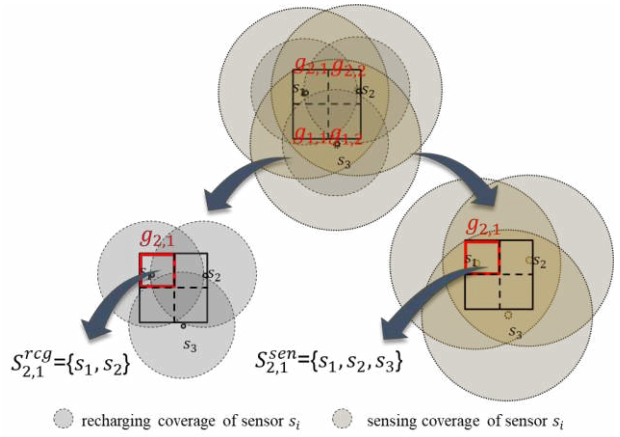

FIGURE 3. **An example to illustrate $S_{2,1}^{rcg}$ and $S_{2,1}^{sen}$ of grid $g_{2,1}$.**

B. RECHARGING SCHEDULING PHASE

This phase aims to choose a few sensors, which have sent the recharging requests to M to be recharged. Then the selected sensors will be scheduled for recharging. Two algorithms are proposed in this phase. The first one is the *Cost-Effective* (*CE*) *algorithm* while the second one is *Cost-Effective with Consideration of Coverage and Fairness* (C^2F) *algorithm.*

1) COST-EFFECTIVE (CE) ALGORITHM

The *CE algorithm* considers $E_{i,j}^{rem}$ of individual sensor and the movement cost of M. This algorithm aims to choose the best grid for M to execute the recharging operation. Let $g_{x,y}^{best}$ represent the best grid, which is the next visited location for M. Let G_{cover} represent the set of grids that are covered by at least one sensor s_i. For each $g_{x,y} \in G_{cover}$, the next task aims to determine the benefit of $g_{x,y}$ if M moves to $g_{x,y}$ for executing the recharging operation.

Let $s_{i,x,y}^{lowest}$ represent the sensor s_i with the least $E_{i,j}^{rem}$ in $S_{x,y}^{rcg}$. Recall that $S_{x,y}^{rcg}$ represent the recharging coverage set whose recharging range covers $g_{x,y}$. That is,

$$s_{i,x,y}^{lowest} = arg \min_{s_i \in S_{x,y}^{rcg}} E_{i,current}^{rem} \quad (17)$$

The *Cost-Effective algorithm* aims to identify k sensors with the least $E_{i,j}^{rem}$. Let min^k denote the function, which returns the *top-k* lowest remaining energy. Let S^{lowest} denote the set of sensors with the lowest remaining energy in all the grids. The S^{lowest} can be calculated as shown in Exp. (18).

$$S^{lowest} = \left\{ s_{i,x,y}^{lowest} \middle| s_{i,x,y}^{lowest} = arg \min_{1 \le i \le n}^{k} E_{i,current}^{rem} \right\} \forall g_{x,y} \in G_{cover} \quad (18)$$

For each sensor $s_{i,x,y}^{lowest} \in S^{lowest}$, the following operations are executed. Let $T_{i,j,x,y}^{crg}$ denote the time length required for sensor $s_{i,x,y}^{lowest}$ to be fully recharged by M at t_j. The value of $T_{i,j,x,y}^{crg}$ can be evaluated by applying Exp. (19).

$$T_{i,j,x,y}^{crg} = \frac{B - E_{i,j}^{rem}}{E_i^{crg}} \quad (19)$$

It is noticed that sensor $s_{i,x,y}^{lowest}$ continuously consumes energy during the movement of M from $l_{current}$ to $g_{x,y}$. This occurs because that sensor $s_{i,x,y}^{lowest}$ continues to execute the sensing task. Let $T_{current,x,y}^{move}$ represent the time length that M moves from $l_{current}$ to $g_{x,y}$. Recall that the speed of M is v. Exp. (20) can be applied to derive the value of $T_{current,x,y}^{move}$.

$$T_{current,x,y}^{move} = \frac{d(l_{current}, l_{g_{x,y}})}{v} \quad (20)$$

Herein, it should be noticed that sensor $s_{i,x,y}^{lowest}$ continuously consumes energy during $T_{current,x,y}^{move}$. Thus, the total required energy of $s_{i,x,y}^{lowest}$ should be considered including $T_{current,x,y}^{move}$. Let $T_{i,j,x,y}^{total\_crg}$ represent the time length required to completely charge $s_{i,x,y}^{lowest}$ by considering the consumed energy during $T_{current,x,y}^{move}$. The value of $T_{i,j,x,y}^{total\_crg}$ can be calculated by applying Exp. (21).

$$T_{i,j,x,y}^{total\_crg} = T_{i,j,x,y}^{crg} + \frac{T_{current,x,y}^{move} * E_i^{con}}{E_i^{crg}} \quad (21)$$

If M moves to $g_{x,y}$, the energies of all the sensors $s_i \in S_{x,y}^{rcg}$ will be increased. Besides, the sensors $s_k \notin S_{x,y}^{rcg}$ will continuously consume their energies for performing the sensing operation during $T_{i,j,x,y}^{total\_crg}$. To determine the cost for executing the recharging operation in $g_{x,y}$, the remaining lifetime of the sensors $s_k \notin S_{x,y}^{rcg}$ is calculated. Let T_k^{life} represent the remaining lifetime of sensors $s_k \notin S_{x,y}^{rcg}$ starting from the current time point. The value of T_k^{life} can be calculated by Exp. (22).

$$T_k^{life} = \frac{E_{i,j}^{rem}}{E_i^{con}} \quad (22)$$

That is to say, the value of T_k^{life} is calculated based on the remaining lifetime of the sensor s_k. Let $\Phi_{x,y}^{weight}$ represent the weight of $g_{x,y}$, including the remaining lifetime of sensors $s_k \notin S_{x,y}^{rcg}$. Exp. (23) presents the calculation of $\Phi_{x,y}^{weight}$ in terms of T_k^{life}.

$$\Phi_{x,y}^{weight} = \sum_{s_k \notin S_{x,y}^{rcg}} T_k^{life} \quad (23)$$

Let max^k denote the function returning the *top-k* highest weights. The recharging strategy is that M moves to the best *top-k* grids $g_{x,y}^{best}$ such that all sensors $s_k \notin S_{x,y}^{rcg}$ have a maximal lifetime.

Top-k Maximal Lifetime Policy:

$$g_{x,y}^{best} = arg \max_{g_{x,y} \in G_{cover}}^{k} \Phi_{x,y}^{weight} \quad (24)$$

Let grid $g_{x,y}^{best}$ denote the *top-k* best grids which have the

This article has been accepted for publication in a future issue of this journal, but has not been fully edited. Content may change prior to final publication. Citation information: DOI 10.1109/ACCESS.2021.3088524, IEEE Access

maximal weight and will be used to construct the charging path. Exp. (25) reflects the recharging policy.

$$G^{best} = arg \max_{g_{x,y} \in G_{cover}}{}^{k} \; g_{x,y}^{best} \tag{25}$$

Let the set of *top-k* best grids be represented by the ordered list. That is,

$$G^{best} = (g_{x_1,y_1}^{best}, g_{x_2,y_2}^{best}, \dots g_{x_k,y_k}^{best}).$$

Then M will construct a path passing through each grid in G^{best} according to the list order $g_{x_1,y_1}^{best}, g_{x_2,y_2}^{best}, \dots g_{x_k,y_k}^{best}$. The last charged time of the sensor should be taken into account. By considering the fairness of recharging the sensors, if the sensor s_i is charged in t_j, the same sensor s_i should not be charged again in t_j. The simulation results of the *fairness of recharging* are discussed in section V. This strategy helps to avoid the ping-pong effect which is raised by the movement of M. Let $T_{i,j,x,y}^{lock}$ represent the time length that M cannot visit $g_{x,y}$ which has been already recharged in t_j.

Let $\frac{B}{E_i^{con}}$ represent the lifetime of each sensor s_i covering $g_{x,y}$. Let $|S_{x,y}^{rcg}|$ denote the number of sensors covering $g_{x,y}$ and ε is a parameter that calculates the waiting time of $g_{x,y}$ for next visit. Exp. (26) calculates the value of $T_{i,j,x,y}^{lock}$.

$$T_{i,j,x,y}^{lock} = \frac{1}{|S_{x,y}^{rcg}|} \sum_{s_i \in S_{x,y}^{rcg}} \frac{B}{E_i^{con}} / \varepsilon \tag{26}$$

Based on the abovementioned *Top-k Maximal Lifetime* policy, M will select *top-k* best grids to construct the charging path and perform the charging task along the path. Then M will go to the first grid in the constructed path and update $E_{i,j}^{rem}$ of all sensors $s_i \in S$. During the execution of the recharging task, M might receive more recharging requests from other sensors. It will again calculate the next *k*-best $g_{x,y}^{best}$ aiming to recharge the following $s_{i,x,y}^{lowest}$. The calculations of $s_{i,x,y}^{lowest}$, $g_{x,y}^{best}$, $T_{i,j,x,y}^{crg}$, $T_{current,x,y}^{move}$ as well as $T_{i,j,x,y}^{total\_crg}$ will be considered as the operations of each round.

Fig. 4 illustrates the procedure of executing the proposed *CE algorithm*. According to the example shown in Fig. 4, five sensors $S=\{s_1, s_2, s_3, s_4, s_5\}$ are randomly deployed in the given region. Assume that the remaining energy of the five sensors are s_1 =70, s_2 =100, s_3 =100, s_4 =85 and s_5 =80. The grids $g_{4,5}$, $g_{6,4}$ and $g_{7,6}$ are the three candidates to play the role of $g_{x,y}^{best}$. These three grids are the best locations to be visited by M. Assume that the distances between M and the grids $g_{4,5}$, $g_{6,4}$ and $g_{7,6}$ are 1, 2 and 3, respectively. Assume that E_i^{con}=1 and v =1. Furthermore, assume that $E_{i,j}^{crg} = 1$ for all sensor s_i. As shown in Fig. 4, it is obvious that $S_{6,4}^{rcg} = \{s_1, s_2, s_3\}$, $S_{4,5}^{rcg} = \{s_3, s_5\}$ and $S_{7,6}^{rcg} = \{s_2, s_4\}$. The first step is to identify the sensor $s_{i,x,y}^{lowest}$ in each $S_{x,y}^{rcg}$.

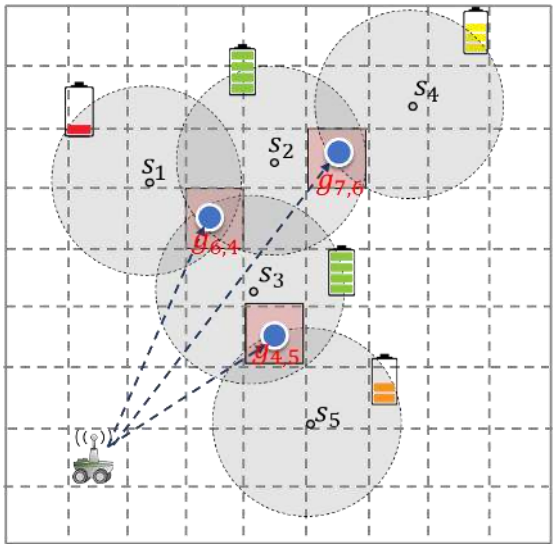

FIGURE 4. **According to the CE algorithm, *M* finds the next visited location.**

In this example, we have $s_{i,6,4}^{lowest} = s_1$ in $S_{6,4}^{rcg}$, $s_{i,4,5}^{lowest} = s_5$ in $S_{4,5}^{rcg}$ and $s_{i,7,6}^{lowest} = s_4$ in $S_{7,6}^{rcg}$. Next, $T_{i,j,x,y}^{crg}$ for each candidate grid $g_{x,y}$ should be calculated. The following takes the grid $g_{6,4}$ as an example to derive the charging location. First, we have

$$T_{1,j,6,4}^{crg} = \frac{B - E_{1,j}^{rem}}{E_1^{crg}} = \frac{100-70}{1} = 30.$$

Next, we have

$$T_{current,6,4}^{move} = \frac{d(l_{current}, l_{g_{6,4}})}{v} = \frac{2}{1} = 2.$$

Therefore, we have

$$T_{1,j,6,4}^{total\_crg} = T_{i,j,x,y}^{crg} + \frac{T_{current,6,4}^{move} * E_1^{con}}{E_1^{rcg}} = 30 + \frac{2*1}{1} = 32$$

According to the fact of $\{ s_k \notin S_{6,4}^{rcg} \} = \{ s_4, s_5 \}$, the following further calculates the remaining lifetime of s_4 and s_5.

$$T_4^{life} = 72 \text{ and } T_5^{life} = 60$$

Finally, it is obtained that the weight of the grid $g_{6,4}$ is 132. Similarly, the weights of the grids $g_{4,5}$ and $g_{7,6}$ are 189 and 187, respectively. According to Exp. (24), the best recharging location is

$$g_{x,y}^{best} = g_{4,5}$$

This implies that M will go to grid $g_{4,5}$ to charge the sensors s_3 and s_5. According to Exp. (25), M constructs the charging path. The procedure of the *CE Algorithm* is detailed below.

Procedure: CE Algorithm

Inputs:

1. $S = \{s_1, s_2, \dots s_i, \dots s_n\}$.
2. B, E_i^{con}, $E_{i,j}^{rem}$, c_i^{sen} and c_i^{rcg} of sensor s_i.
3. The total observing time is $T=\{t_1, t_2, \dots t_j, \dots t_m\}$.

This article has been accepted for publication in a future issue of this journal, but has not been fully edited. Content may change prior to final publication. Citation information: DOI 10.1109/ACCESS.2021.3088524, IEEE Access

Outputs:
1. The monitoring quality Q by all sensors during T.

1. t_j=t_1;
2. **Repeat** {
3. $S_{x,y}^{rcg} = \{s_i | g_{x,y}\ is\ recharging\ covered\ by\ c_i^{rcg}\}$;
4. $s_{i,x,y}^{lowest} = arg \min_{s_i \in S_{x,y}^{rcg}} E_{i,current}^{rem}$;
5. $S^{lowest} = \left\{ s_{i,x,y}^{lowest} \middle| s_{i,x,y}^{lowest} = arg \min_{1 \le i \le n}^{k} E_{i,current}^{rem} \right\} \forall g_{x,y} \in G_{cover}$;
6. $T_{i,j,x,y}^{crg} = \frac{B - E_{i,j}^{rem}}{E_i^{crg}}$;
7. $T_{current,x,y}^{move} = \frac{d(l_{current}, l_{g_{x,y}})}{v}$;
8. $T_{i,j,x,y}^{total\_crg} = T_{i,j,x,y}^{crg} + \frac{T_{current,x,y}^{move} * E_i^{con}}{E_i^{crg}}$;
9. $T_k^{life} = \frac{E_{i,j}^{rem}}{E_i^{con}}$;
10. $g_{x,y}^{best} = arg \max_{g_{x,y} \in G_{cover}}^{k} \Phi_{x,y}^{weight}$;
11. The M will go to the grid $g_{x,y}^{best}$ to charge
12. $l_{current}$= =$l_{g_{x,y}}$;
13. Update $E_{i,j}^{rem}$ of $s_i \in S$;
14. **Until** (t_j= =t_m) }
15. Compute Q in T according to Exp. (7);
16. **Return** Q;

2) COST-EFFECTIVE WITH CONSIDERATION OF COVERAGE AND FAIRNESS (C^2F) ALGORITHM

The C^2F *algorithm* further considers the obtained loss and benefits before the calculation of every possible recharging location. Let $g_{x,y}$ represent the candidate recharging location where $s_i \in S_{x,y}^{rcg}$ will be charged. The C^2F *algorithm* considers two benefits when M goes to $g_{x,y}$ to execute the recharging operation. The first benefit is considering the *chain-effect* while the second one is calculating the coverage loss and benefits of each candidate charging location.

The following will discuss the benefit and weight of recharging each sensor $s_i \in S_{x,y}^{rcg}$. Let $\Phi_{x,y}^{benefit}$ denote the benefit obtained from recharging $s_i \in S_{x,y}^{rcg}$. The value of $\Phi_{x,y}^{benefit}$ can be measured by Exp. (27).

$$\Phi_{x,y}^{benefit} = \frac{\sum_{s_i \in S_{x,y}^{rcg}} E_i^{crg} \times \bigcup_{s_i \in S_{x,y}^{rcg}} c_i^{sen}}{\left| S_{x,y}^{rcg} \right|} \quad (27)$$

As shown in Exp. (27), two benefits, including the total recharged energy and the coverage contribution, are obtained by recharging the sensors $s_i \in S_{x,y}^{rcg}$ at grid $g_{x,y}$. Since the $\Phi_{x,y}^{benefit}$ denotes the average benefit obtained from $s_i \in S_{x,y}^{rcg}$, the total benefit is divided by $\left| S_{x,y}^{rcg} \right|$.

The distance between the current location of M and $g_{x,y}$ is considered as the cost if M moves to $g_{x,y}$. Recall that $d(l_a, l_b)$ represents the distance between l_a and l_b. The $\Phi_{x,y}^{weight}$ of grid $g_{x,y}$ is the average benefit, which is divided by $d(l_a, l_b)$, as shown in Exp. (28).

$$\Phi_{x,y}^{weight} = \Phi_{x,y}^{benefit} / d(l_a, l_b) \quad (28)$$

Let grid G^{best} denote the set of *top-k* best grids which have the maximal weight and will be used to construct the charging path. Exp. (29) reflects the recharging policy.

$$G^{best} = arg \max_{g_{x,y} \in G_{cover}}^{k} \Phi_{x,y}^{weight} \quad (29)$$

Let the set of *top-k* best grids be represented by the ordered list. We have,

$$G^{best} = (g_{x_1,y_1}^{best}, g_{x_2,y_2}^{best}, \dots g_{x_k,y_k}^{best}).$$

Then M will construct a path passing through each grid in G^{best} according to the list order $g_{x_1,y_1}^{best}, g_{x_2,y_2}^{best}, \dots g_{x_k,y_k}^{best}$. To maintain the fairness of recharging the sensors, all the recharged sensors will be locked $T_{i,j,x,y}^{lock}$ as shown in Exp. (26). This policy helps M to avoid the ping-pong effect, which is caused by the movement of M. The following presents the recharging policy.

Fairness Recharging Policy:

Assume that g_{x_1,y_1}^{best} is considered as the recharging location at t_j. Then g_{x_1,y_1}^{best} will be locked for T_{i,j,x_1,y_1}^{lock} and M will visit g_{x_1,y_1}^{best} only after $t_j + T_{i,j,x_1,y_1}^{lock}$.

Based on the abovementioned *Top-k Charging Fairness* policy, M will select *top-k* best grids to construct the charging path and perform the charging task along the path. The path construction issue will be discussed in the next subsection. Then M will go to the first grid in the constructed path and update $E_{i,j}^{rem}$ of all sensors $s_i \in S$. During the execution of the recharging task, M might receive more recharging requests from other sensors. Therefore, it will again calculate the next *k*-best $g_{x,y}^{best}$ grids, aiming to visit the next $g_{x,y}^{best}$. The calculations of $\Phi_{x,y}^{benefit}$, $\Phi_{x,y}^{weight}$ as well as G^{best} will be executed in each round.

Fig. 5 illustrates the procedure of executing the proposed C^2F *algorithm*. According to the example shown in Fig. 5, there are five sensors S=$\{s_1, s_2, s_3, s_4, s_5\}$ deployed in the monitoring region. The grids $g_{4,5}$, $g_{6,4}$ and $g_{7,6}$ are the three candidates to play the role of $g_{x,y}^{best}$. These three grids are the best locations to be visited by M. Assume that the distances between M and the grids $g_{4,5}$, $g_{6,4}$, and $g_{7,6}$ are 1, 2 and 3, respectively. Therefore, we

$S_{6,4}^{rcg} = \{s_1, s_2, s_3\}$, $S_{4,5}^{rcg} = \{s_3, s_5\}$ and $S_{7,6}^{rcg} = \{s_2, s_4\}$

Assume that we have,

$\sum_{s_i \in S_{6,4}^{rcg}} E_i^{crg} = 3.5$, $\sum_{s_i \in S_{4,5}^{rcg}} E_i^{crg} = 3$ and

$\sum_{s_i \in S_{7,6}^{rcg}} E_i^{crg} = 3$

Also, assume that we have

This article has been accepted for publication in a future issue of this journal, but has not been fully edited. Content may change prior to final publication. Citation information: DOI 10.1109/ACCESS.2021.3088524, IEEE Access

$$\bigcup_{s_i \in S_{6,4}^{rcg}} c_i^{sen} = 100, \bigcup_{s_i \in S_{4,5}^{rcg}} c_i^{sen} = 80, \bigcup_{s_i \in S_{7,6}^{rcg}} c_i^{sen} = 80$$

Therefore, $\Phi_{x,y}^{benefit}$ for each $g_{4,5}, g_{6,4}$ and $g_{7,6}$ can be calculated by:

$$\Phi_{6,4}^{benefit} = \frac{\sum_{s_i \in S_{6,4}^{rcg}} E_i^{crg} \times \bigcup_{s_i \in S_{6,4}^{rcg}} c_i^{sen}}{|S_{6,4}^{rcg}|} = \frac{3.5 \times 100}{3} = 116.67$$

$$\Phi_{4,5}^{benefit} = \frac{\sum_{s_i \in S_{4,5}^{rcg}} E_i^{crg} \times \bigcup_{s_i \in S_{4,5}^{rcg}} c_i^{sen}}{|S_{4,5}^{rcg}|} = \frac{3 \times 80}{2} = 120$$

$$\Phi_{7,6}^{benefit} = \frac{\sum_{s_i \in S_{7,6}^{rcg}} E_i^{crg} \times \bigcup_{s_i \in S_{7,6}^{rcg}} c_i^{sen}}{|S_{7,6}^{rcg}|} = \frac{3 \times 80}{2} = 120$$

Next, the $\Phi_{x,y}^{weight}$ for each $g_{4,5}$, $g_{6,4}$ and $g_{7,6}$ can be calculated by:

$$\Phi_{6,4}^{weight} = \frac{\Phi_{6,4}^{benefit}}{d(l_{current}, l_{6,4})} = \frac{116.67}{2} = 58.3$$

$$\Phi_{4,5}^{weight} = \frac{\Phi_{4,5}^{benefit}}{d(l_{current}, l_{4,5})} = \frac{120}{1} = 120$$

$$\Phi_{7,6}^{weight} = \frac{\Phi_{7,6}^{benefit}}{d(l_{current}, l_{7,6})} = \frac{120}{3} = 40$$

Assume that k=1. According to Exp. (29), the *top*-1 best recharging location is

$$g_{x,y}^{best} = g_{4,5}.$$

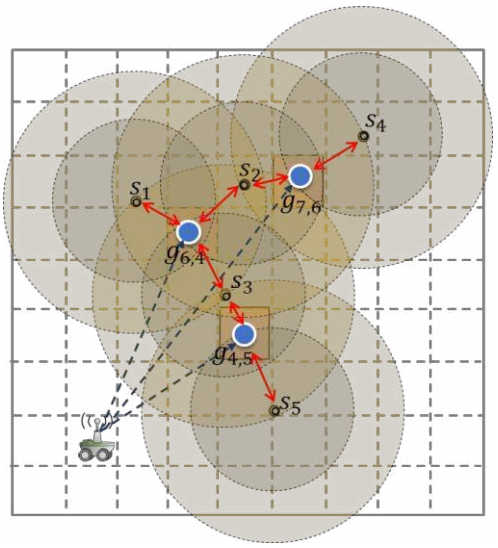

FIGURE 5. **According to the C²F algorithm, M chooses the next $g_{x,y}^{best}$.**

This implies that M will go to the grid $g_{4,5}$ to charge the sensors s_3 and s_5. After completing the charging task, M will not charge the same sensors s_3 and s_5 at the grid $g_{4,5}$ for a time length of 100/ ε. The following summarizes the proposed C^2F *algorithm*.

Procedure: C^2F Algorithm

Inputs:
1. $S = \{s_1, s_2, \ldots s_i, \ldots s_n\}$.
2. $B, E_i^{con}, E_{i,j}^{rem}, c_i^{sen}$ and c_i^{rcg} of sensor s_i.
3. The total observing time is T=$\{t_1, t_2, \ldots t_j, \ldots t_m\}$.

Outputs:
1. The monitoring quality Q by all sensors during T.

1. t_j=t_1;
2. **Repeat** {
3. $S_{x,y}^{rcg} = \{s_i | g_{x,y}$ *is recharging covered by* $c_i^{rcg}\}$;
4. $\Phi_{x,y}^{benefit} = \frac{\sum_{s_i \in S_{x,y}^{rcg}} E_i^{crg} \times \bigcup_{s_i \in S_{x,y}^{rcg}} c_i^{sen}}{|S_{x,y}^{rcg}|}$;
   $\Phi_{x,y}^{weight} = \Phi_{x,y}^{benefit} / d(l_a, l_b)$
   $G^{best} = arg \max_{g_{x,y} \in G_{cover}}^{k} \Phi_{x,y}^{weight}$
5. The M will go to the grid $g_{x,y}^{best}$ to charge
6. $l_{current}$= =$l_{g_{x,y}}$;
7. Update $E_{i,j}^{rem}$ of $s_i \in S$;
8. **Until** (t_j= =t_m) }
9. Compute Q in T according to Exp. (7);
10. **Return** Q;

C. PATH CONSTRUCTION PHASE

In this phase, M will construct a recharging path according to the schedule of sensors in the second phase. Recall that Exps. (24) and (29) return *top-k* best grids to be visited by M. Let the set of *top-k* best grids be an ordered list $G^{best} = (g_{x_1,y_1}^{best}, g_{x_2,y_2}^{best}, \ldots g_{x_k,y_k}^{best})$. The M will construct a path

$$G^{current} = (g_{x_1,y_1}^{best}, g_{x_2,y_2}^{best}, \ldots g_{x_k,y_k}^{best})$$

which passes through each g_{x_i,y_i}^{best} of $G^{current}$. According to the visited order, M will move from $l_{current}$ to the first best grid g_{x_1,y_1}^{best} and then recharge those sensors $s_i \in S_{x_1,y_1}^{rcg}$. During the execution of this recharging task, some other sensors might send recharging requests to M. Then M will consider these requests and execute the proposed algorithms as shown in Phase 2. Then it will construct a new path by applying the Path Construction Phase as proposed in this subsection. The flow chart of the proposed algorithms is shown in Fig. 6.

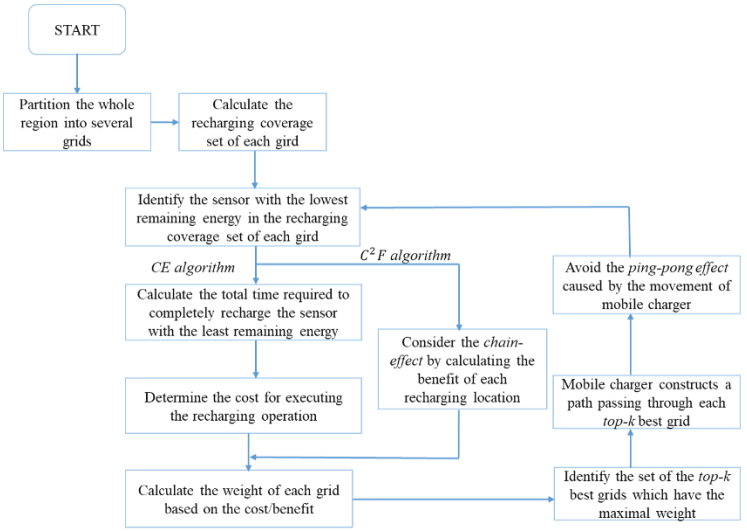

FIGURE 6. **The flowchart of the proposed CE and C²F algorithms.**

This article has been accepted for publication in a future issue of this journal, but has not been fully edited. Content may change prior to final publication. Citation information: DOI 10.1109/ACCESS.2021.3088524, IEEE Access

V. PERFORMANCE EVALUATION

The performance of the proposed *CE* and C^2F against the existing *SDT* and *HSA-DFWA* algorithms is evaluated in this section. Existing study [18] proposed an algorithm *SDT* which investigated the scheduling issue and aimed to maximize the average coverage ratio of WSNs. Another existing study [19] proposed an energy recharging algorithm *HSA-DFWA* by considering the charging time of sensor nodes.

A. SIMULATION SETTINGS

The MATLAB platform is used in the simulation. The number of sensors ranges from 300 to 700. A random deployment of sensors is considered in the monitoring region of size 700m x 700m. The grid size is set at 4m, 7m, 12m, 15m and 18m. The sensing radius of each sensor varies ranging from 5m to 25m. The total energy $E_{charger}^{total}$ of the mobile charger is set at 2000J and the speed v of the mobile charger is set at 5m/s. The total energy consumption E^{move} of mobile charger for moving is set at 0.1J/m. The transmission power P_{crg}^{tx} of the mobile charger is 100J. The initial energy of each sensor is set at 100J.The simulation parameters are listed in Table 2.

TABLE II
SIMULATION PARAMETERS

Parameters	Values
Tool	Matlab
Deployment type	Random
Area size	700m x 700m
Number of sensors	300 - 700
Grid size	4m,7m,12m,15m,18m
Sensing range of sensors	5m−25m
Total energy of mobile charger	2000J
Speed of mobile charger	5m/s
Total energy consumption for movement of mobile charger	0.1J/m
Transmission power	100J
Initial energy of sensor	100J

B. SIMULATION RESULTS

Fig. 7 illustrates the recharging path constructed by the mobile charger adopting the *CE* and C^2F algorithms. As shown in Fig. 7 (a), the size of monitoring region is set at 700m x 700m. In this simulation, the number of deployed sensors is set at 150. The sensing and charging ranges of each sensor are set at 20m and 10m, respectively. The energy of sensors is set at four levels. The red colour sensors represent the sensors with 25% of the remaining energy. Similarly, the yellow, blue and green colour sensors represent the sensors with 50%, 75% and 100% of remaining energies, respectively. Initially, the proposed *CE* algorithm identifies the grids with the sensors, which have the lowest remaining energy. Based on the weight of the grid the best recharging location is determined. According to the simulation shown in Fig. 7 (a), the weight of the grid $g_{7,3}$ is larger. Thus, the mobile charger travels to grid $g_{7,3}$ for recharging the sensors in the charging range of grid $g_{7,3}$ and all the other grids are visited accordingly. The simulation settings of Fig. 7 (b) are similar to Fig. 7 (a). Similar to the *CE* algorithm, the proposed C^2F algorithm identifies the coverage loss and benefit of visiting each grid, which is covered by those waiting recharging sensors. The proposed C^2F algorithm determines the benefit of each recharging location. According to the simulation shown in Fig. 7 (b), the benefit of the grid $g_{4,4}$ is larger. Therefore, the mobile charger moves to the grid $g_{4,4}$ to recharge the sensors and all the other grids are visited accordingly. Finally, the constructed path of the *CE* algorithm is longer as compared to the C^2F algorithm.

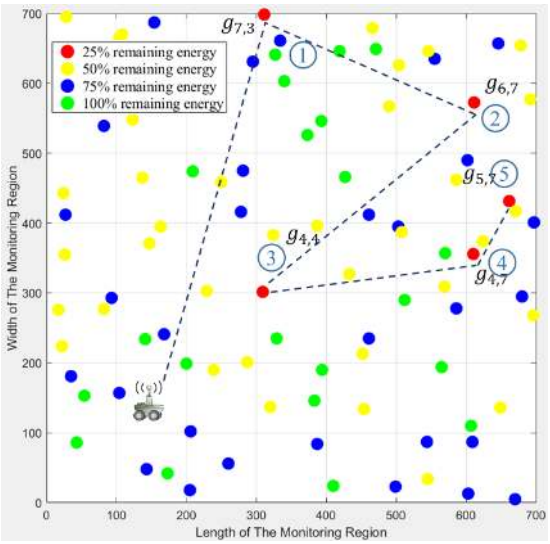

(a) The recharging path constructed by mobile charger adopting the *CE* algorithm

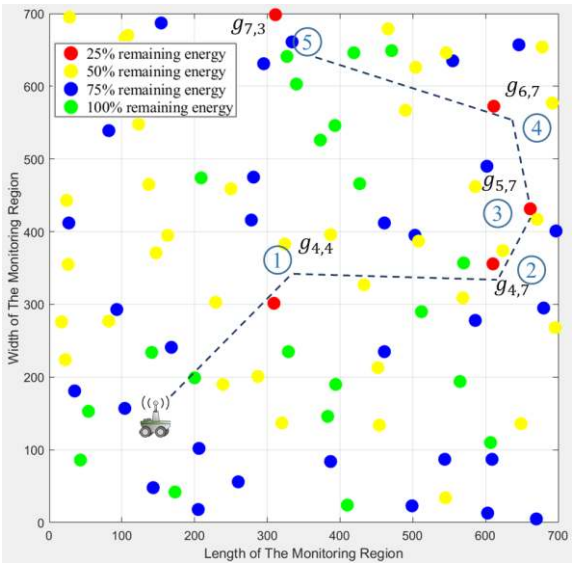

(b) The recharging path constructed by mobile charger adopting the C^2F algorithm

FIGURE 7. **An experiment illustrating the recharging path construction of CE and C^2F algorithms.**

This article has been accepted for publication in a future issue of this journal, but has not been fully edited. Content may change prior to final publication. Citation information: DOI 10.1109/ACCESS.2021.3088524, IEEE Access

Fig. 8 compares the surveillance qualities of C^2F, *CE*, *HSA-DFWA* and *SDT* algorithms by changing the number of sensors and the sensing range. In this simulation, the number of deployed sensors is set at 300 to 700 and the sensing range is adjusted between $5m$ and $25m$. Fig. 8 depicts that, the surveillance quality of all the algorithms increases with the number of deployed sensors. This occurs because if the deployed sensors are more, more sensors have the opportunity to monitor the region. Consequently, it leads to higher surveillance quality. A sensor with a larger sensing radius can cover a larger area, therefore the surveillance qualities of all algorithms increase with sensing radius. The C^2F yields the best performance as compared to the other three algorithms. This is because the C^2F selects the sensors which have larger contributions, leading to a higher surveillance quality. Besides, the existing *SDT* algorithm has lower results compared to C^2F, *CE*, *HSA-DFWA*. This occurs because the *SDT* algorithm divides the sensors into different clusters and charges each cluster separately. The major policy of the *SDT* algorithm is recharging all the sensors in one cluster. It considers the distance between each sensor in the cluster. However, there might be sensors located very closer. Therefore, this policy leads to lower surveillance quality.

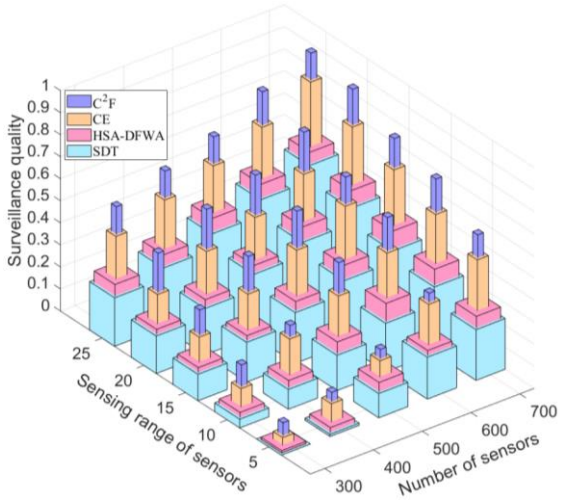

FIGURE 8. **Performance comparison of surveillance quality for C^2F, CE, HSA-DFWA and SDT algorithms.**

Fig. 9 depicts the effect of grid size and sensing range on the surveillance quality. The sensing range and grid size are set from $5m$ to $25m$ and $4m$ to $18m$, respectively. As shown in Fig. 9, the surveillance qualities decrease with grid size and increase with the sensing range. This is because more sensors can effectively cover a smaller grid size. In comparison, the proposed C^2F outperforms the *CE, HSA-DFWA* and *SDT* algorithms. The C^2F algorithm adopts the *charging fairness policy* and determines the obtained loss and benefits of each charging location. Consequently, the larger sensing range and the smaller grid size result in higher surveillance quality.

Fig. 10 evaluates the surveillance qualities by using different deployment policies such as centralized, random and uniform. The number of deployed sensors is set ranging from 300 to 700. As shown in Fig. 10, the uniform policy outperforms the other two policies.

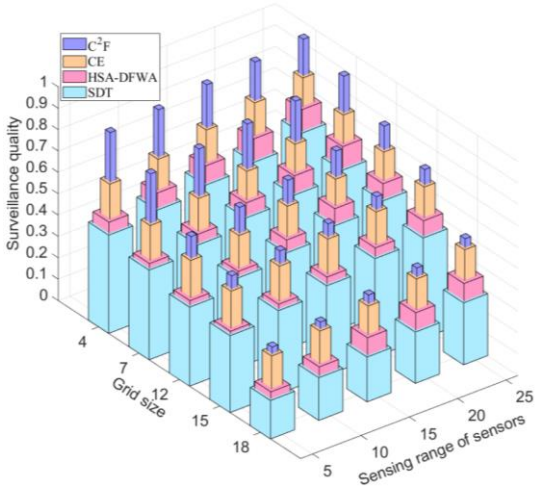

FIGURE 9. **Performance comparison of surveillance quality for C^2F, CE, HSA-DFWA and SDT algorithms.**

In fact, the uniform deployment of sensors performs their task uniformly, which is impractical in the real world. Besides, the C^2F algorithm yields the best performance compared to *CE*, *HSA-DFWA* and *SDT* algorithms specifically for random policy. The two benefits are taken into account by the C^2F algorithm. The increased energy of each sensor and the coverage contribution. This policy helps C^2F algorithm yield the best performance.

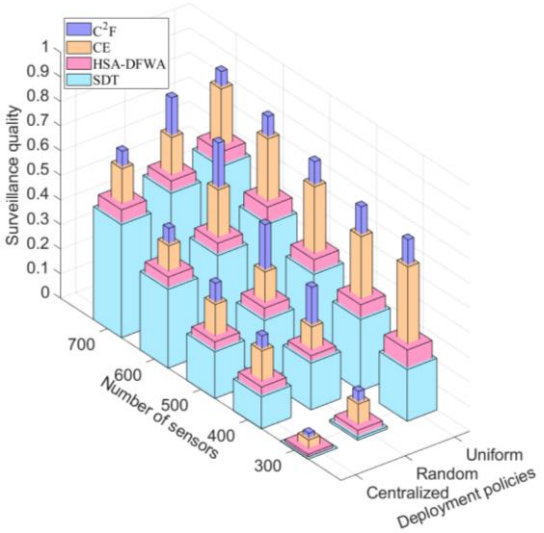

FIGURE 10. **Performance comparison of surveillance quality for C^2F, CE, HSA-DFWA and SDT algorithms.**

Fig. 11 further investigates the fairness index of recharging for C^2F, *CE*, *HSA-DFWA* and *SDT* algorithms by varying the grid size. The grid size is adjusted from $4m$ to $18m$ and the number of deployed sensors is set at 700 and 600. In this experiment, the energy of each sensor is set at 15000 units. The recharging fairness index is calculated according to Exp. (30).

This article has been accepted for publication in a future issue of this journal, but has not been fully edited. Content may change prior to final publication. Citation information: DOI 10.1109/ACCESS.2021.3088524, IEEE Access

$$Fairness\ Index = \frac{(\sum_{i=1}^{n} x_i)^2}{n * \sum_{i=1}^{n} x_i^2} \quad (30)$$

where x_i denotes the recharged energy of the sensor node s_i. Fig. 11 depicts that C^2F and *CE* algorithms yield better performance than *HSA-DFWA* and *SDT* algorithms. This is because that C^2F algorithm determines coverage contribution of the individual sensor. Besides, both C^2F, *CE* algorithms avoid the ping-pong effect caused by the movement of M. This policy helps M to recharge more sensors, which improves the fairness index value.

Fig. 12 evaluates the data quality of the recharged sensors. Since the deployed sensors are more and recharging each sensor is time-consuming, a mobile charger is usually unable to recharge all sensors. In this case, the recharged sensors are expected to be distributed all over the area. Herein, the data quality represents the degree that the collected data of sensors can represent the data of the whole monitoring region.

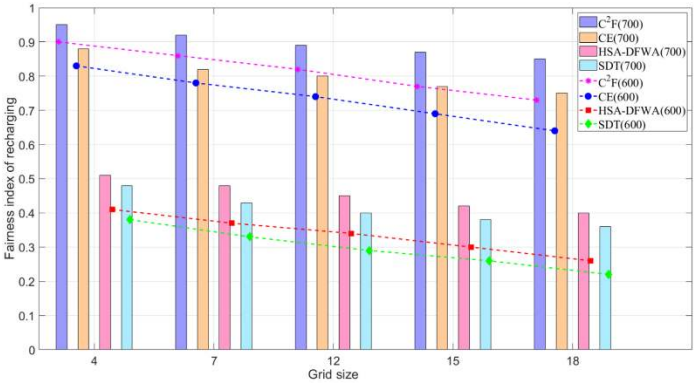

FIGURE 11. **Performance comparison of fairness index of recharging for C^2F , CE, HSA-DFWA and SDT algorithms by varying the grid size.**

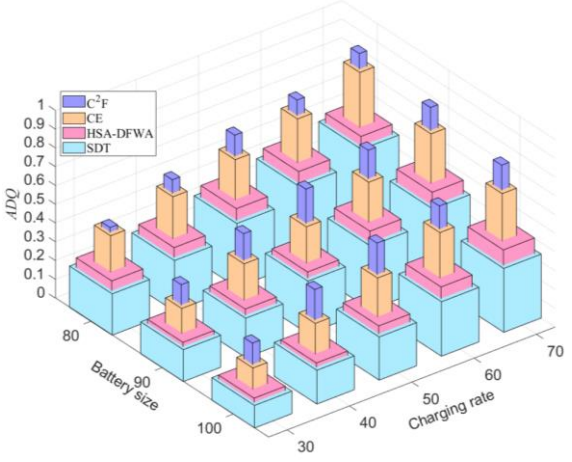

FIGURE 12. **Performance comparison of ADQ of recharged sensors by varying the charging rate and the battery size.**

Let $\hat{S}=\{\hat{s}_1, \hat{s}_2, \ldots \hat{s}_i, \ldots \hat{s}_x\}$ denote the set of x recharged sensors in each round. If the x sensors can be equally distributed over the whole monitoring region, their Voronoi cells will have a similar size. In the other case, if the x sensors are closely located to each other, their Voronoi cells will have different sizes. The area size of the Voronoi cell of the sensor $\hat{s}_i$ indicates that the environmental data occurred in that cell area can be represented by the data collected by the sensor $\hat{s}_i$. Therefore, a small cell size indicates that the collected data can better represent the corresponding cell region. That is to say, if all cell sizes are similar, the maximal cell size can be minimized. This also implies that the data collected by the x sensors have higher data quality. Let the Voronoi cells in the monitoring region be denoted by $C = \{C_1, C_2, \ldots . . C_x\}$. Let ξ_i be the cell size of C_i. The Average Data Quality (*ADQ*) of the recharged sensors is calculated by applying Exp. (31).

$$ADQ = \frac{\left(\sum_{i=1}^{x} \xi_i\right)^2}{x * \sum_{i=1}^{x} \xi_i^2} \quad (31)$$

Fig. 12 compares the data quality of C^2F, *CE*, *HSA-DFWA* and *SDT* algorithms in terms of charging rate and battery size. The charging rate and the battery size varied from 30 to 70 units and 80 to 100, respectively. Fig. 12 illustrates that the data quality of C^2F, *CE*, *HSA-DFWA* and *SDT* algorithms increase with the charging rate. This occurs because mobile charger can recharge more sensors. Consequently, it leads to the higher data quality of recharged sensors. Besides, the data quality of the four algorithms decreases with battery size. This occurs because the sensors need to be recharged for a long time when the battery size is enlarged. In comparison, C^2F and *CE* algorithms outperform the *HSA-DFWA* and *SDT* algorithms. This occurs because C^2F and *CE* algorithms avoid the ping-pong effect. This strategy helps recharge a larger number of sensors without incurring many detours, leading to higher data quality.

Fig. 13 investigates the performance of recharging stability for C^2F, *CE*, *HSA-DFWA* and *SDT* algorithms. To conduct this experiment, nine random locations are observed in the monitoring region. The considered monitoring region size is 700m * 700m and the number of sensors is 2000. The sensing range of each sensor is set at 20m. The proposed C^2F algorithm achieves the best recharging stability compared to the *HSA-DFWA* and *SDT* algorithms. The C^2F algorithm determines the benefit of each grid before every charging decision. It also adopts the *charging fairness policy*, which helps M to avoid the ping-pong effect.

Fig. 14 compares the coverage ratio of four algorithms in terms of deployed sensors and sensing range. The number of deployed sensors is varied ranging from 300 to 700 and the sensing range is adjusted between 5m and 25m. As shown in Fig. 14, the coverage ratio grows with both the deployed sensors and the sensing range. This occurs because that more sensors can enlarge the coverage area and hence have a larger coverage contribution. Besides, sensors with a large sensing range can cover larger region.

This article has been accepted for publication in a future issue of this journal, but has not been fully edited. Content may change prior to final publication. Citation information: DOI 10.1109/ACCESS.2021.3088524, IEEE Access

Therefore, the quality of the monitoring region is increased, leading to a higher coverage ratio. In comparison, C^2F outperforms *CE*, *HSA-DFWA* and *SDT* algorithms. This occurs because that the proposed C^2F selects the sensors based on the coverage contribution.

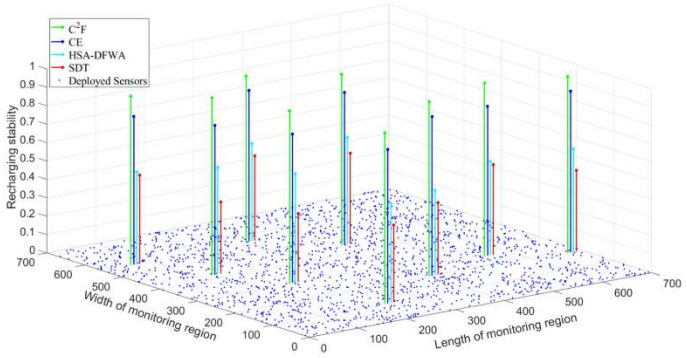

FIGURE 13. **Comparison of recharging stability of C^2F , CE, HSA-DFWA and SDT algorithms.**

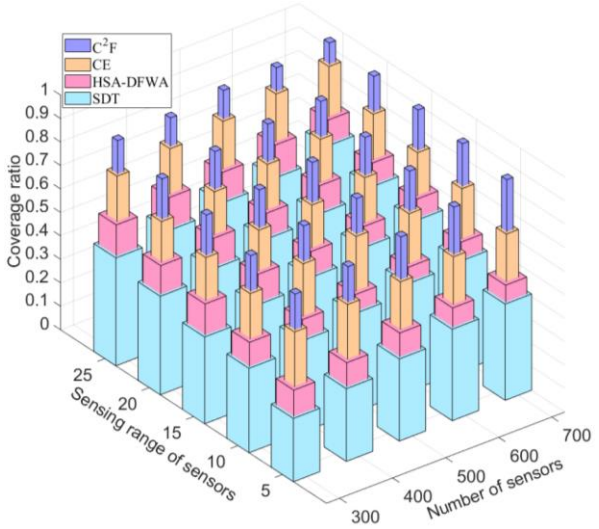

FIGURE 14. **Performance comparison of coverage ratio for C^2F , CE, HSA-DFWA and SDT algorithms.**

VI. CONCLUSIONS

This paper proposed an energy-recharging algorithm aiming to maximize the accumulated monitoring quality of all the sensors in the given region. The proposed algorithm consists of three phases: *Initialization Phase, Recharging Scheduling Phase* and *Path Construction Phase*. The first phase calculates $S_{x,y}^{rcg}$ and $S_{x,y}^{sen}$ of each $g_{x,y}$. After that, the second phase aims to select some sensors, which have sent the recharging requests to M to be recharged. Finally, the third phase constructs a charging path according to the schedule of sensors in the second phase. This paper proposed two recharging algorithms, including the *CE* and C^2F. Firstly, the *CE* algorithm determines the cost of each recharging operation executed by M and considers the *Top-k Maximal Lifetime* policy. The C^2F algorithm further considers both the obtained loss and benefits before the calculation of every recharging location. Performance evaluation shows that the proposed *CE* and C^2F algorithms outperform the existing *HSA-DFWA* and *SDT* algorithm in terms of fairness index of recharging, recharging stability and coverage ratio.

The issue of multiple mobile chargers and their cooperation such as task partitioning will be considered as the future work of this study. Furthermore, we would like to relax the constraints of this paper.

REFERENCES

[1] H. Mostafaei, M. U. Chowdhury, and M. S. Obaidat, "Border surveillance with WSN systems in a distributed manner," *IEEE System Journal*, vol. 12, no. 4, pp. 3703-3712, Dec. 2018.

[2] A. Alaiad and L. Zhou, "Patient's Adoption of WSN-Based Smart Home Healthcare Systems: An Integrated Model of Facilitators and Barriers," *IEEE Transactions on Professional Communication*, vol. 60, no. 1, pp. 4-23, Mar. 2017.

[3] O. Gulec, E. Haytaoglu and S. Tokat, "A Novel Distributed CDS Algorithm for Extending Lifetime of WSNs with Solar Energy Harvester Nodes for Smart Agriculture Applications," *IEEE Access*, vol. 8, pp. 58859-58873, Mar. 2020.

[4] W. Liao, B. Dande, C. Chang and D. S. Roy, "MMQT: Maximizing the Monitoring Quality for Targets Based on Probabilistic Sensing Model in Rechargeable Wireless Sensor Networks," *IEEE Access*, vol. 8, pp. 77073-77088, Apr. 2020.

[5] C. Xu, Z. Xiong, G. Zhao and S. Yu, "An Energy-Efficient Region Source Routing Protocol for Lifetime Maximization in WSN," *IEEE Access*, vol. 7, pp. 135277-135289, Sep. 2019.

[6] S. Siddiqui, S. Ghani and A. A. Khan, "ADP-MAC: An Adaptive and Dynamic Polling-Based MAC Protocol for Wireless Sensor Networks," *IEEE Sensors Journal*, vol. 18, no. 2, pp. 860-874, Jan. 2018.

[7] A. L. Prasanna, V. Kumar and S. B. Dhok, "Cooperative Communication and Energy-Harvesting-Enabled Energy-Efficient Design of MI-Based Clustered Nonconventional WSNs," *IEEE Systems Journal*, vol. 14, no. 2, pp. 2293-2302, Jun. 2020.

[8] L. -. Hung, F. -. Leu, K. -. Tsai and C. -. Ko, "Energy-Efficient Cooperative Routing Scheme for Heterogeneous Wireless Sensor Networks," *IEEE Access*, vol. 8, pp. 56321-56332, Mar. 2020.

[9] H. Sharma, A. Haque and Z. A. Jaffery, "An Efficient Solar Energy Harvesting System for Wireless Sensor Nodes," in *Proc. IEEE 2nd International Conference on Power Electronics, Intelligent Control and Energy Systems (ICPEICES)*, Delhi, India, Oct. 2018, pp. 461-464.

[10] Y. Peng, W. Qiao, L. Qu and J. Wang, "Sensor Fault Detection and Isolation for a Wireless Sensor Network-Based Remote Wind Turbine Condition Monitoring System," *IEEE Transactions on Industry Applications*, vol. 54, no. 2, pp. 1072-1079, March-April 2018.

[11] F. Deng, X. Yue, X. Fan, S. Guan, Y. Xu and J. Chen, "Multisource Energy Harvesting System for a Wireless Sensor Network Node in the Field Environment," *IEEE Internet of Things Journal*, vol. 6, no. 1, pp. 918-927, Feb. 2019.

[12] K. Liu, J. Peng, L. He, J. Pan, S. Li, M. Ling, and Z. Huang, "An active mobile charging and data collection scheme for clustered sensor networks," *IEEE Trans. Veh. Technol.*, vol. 68, no. 5, pp. 5100-5113, Mar. 2019.

[13] Z. Lyu, Z. Wei, J. Pan, H. Chen, C. Xia, J. Han, and L. Shi, "Periodic charging planning for a mobile WCE in wireless rechargeable sensor networks based on hybrid PSO and GA algorithm," *Appl. Soft Comput.*, vol. 75, no. 1, pp. 388-403, Feb. 2019.

[14] H. Dai *et al.*, "CHASE: Charging and Scheduling Scheme for Stochastic Event Capture in Wireless Rechargeable Sensor Networks," *IEEE Transactions on Mobile Computing*, vol. 19, no. 1, pp. 44-59, 1 Jan. 2020.

[15] W. Xu,W. Liang, X. Jia, Z. Xu, Z. Li, and Y. Liu, "Maximizing sensor lifetime with the minimal service cost of a mobile charger in wireless

sensor networks," *IEEE Trans. Mobile Comput*., vol. 17, no. 11, pp. 2564-2577,Nov. 2018.

[16] A. Tomar and P. K. Jana, "Designing energy efficient traveling paths for multiple mobile chargers in wireless rechargeable sensor networks," *Tenth International Conference on Contemporary Computing* (IC3), Noida, India, 2017, pp. 1-6.

[17] A. Tomar, L. Muduli and P. K. Jana, "A Fuzzy Logic-based On-demand Charging Algorithm for Wireless Rechargeable Sensor Networks with Multiple Chargers," *IEEE Transactions on Mobile Computing*.

[18] H. Huang, S. Lin, L. Chen, J. Gao, A. Mamat and J. Wu, "Dynamic Mobile Charger Scheduling in Heterogeneous Wireless Sensor Networks," in *Proc. IEEE 12th International Conference on Mobile Ad Hoc and Sensor Systems*, Dallas, TX, USA, Oct. 2015, pp. 379-387.

[19] Z. Lyu et al., "Multi-Node Charging Planning Algorithm With an Energy-Limited WCE in WRSNs," *IEEE Access*, vol. 7, pp. 47154-47170, Apr. 2019.

[20] J. A. Shaw, "Radiometry and the Friis transmission equation," *Amer. J. Phys*., vol. 81, no. 1, pp. 33–37, Sep. 2013.